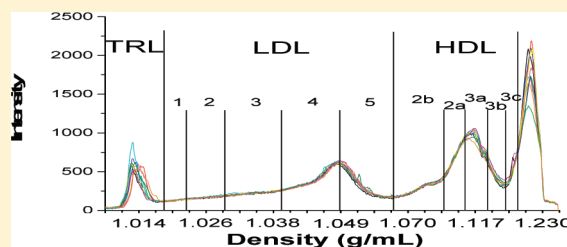


# Developing High Performance Lipoprotein Density Profiling for Use in Clinical Studies Relating to Cardiovascular Disease

Craig D. Larner, Ronald R. Henriquez, Jeffrey D. Johnson, and Ronald D. Macfarlane\*

Department of Chemistry, Texas A&M University, 3255 TAMU, College Station, Texas 77843-3255, United States

**ABSTRACT:** Early detection of the beginning stage of cardiovascular disease (CVD) is an approach to prevention because the process is reversible at this stage. Consequently, several methods for screening for CVD have been introduced in recent years incorporating different analytical methods for characterizing the population of blood-borne lipoprotein subclasses. The gold standard method for lipoprotein subclassification is based on lipoprotein density measured by sedimentation equilibrium using the ultracentrifuge. However, this method has not been adopted for clinical studies because of difficulties in achieving the precision required for distinguishing individuals with and without CVD particularly when statistical classification methods are used. The objective of this study was to identify and improve the major factors that influence the precision of measurement of lipoprotein density profile by sedimentation equilibrium analysis and labeling with a fluorescent probe. The study has two phases, each contributing to precision. The first phase focuses on the ultracentrifugation-related variables, and the second phase addresses those factors involved in converting the fluorescent lipoprotein density profile to a digital format compatible with statistical analysis. The overall improvement in precision was on the order of a factor of 5, sufficient to be effectively applied to ongoing classification studies relating to CVD risk assessment.



Cardiovascular disease (CVD) is a leading cause of death in the world today. The need for a precise and repeatable method for accurately measuring and quantifying the lipoprotein density profile for studies dealing with CVD is necessary for screening, prediction of disease, and possibly monitoring the effectiveness of treatment.<sup>1–5</sup> Several years ago, recognizing the contribution that modern methods of analytical chemistry can contribute to supporting medical research and new healthcare initiatives, we formed a “laboratory for cardiovascular chemistry”. We selected capillary electrophoresis,<sup>6–8</sup> density gradient ultracentrifugation (DGU),<sup>9–12</sup> and mass spectrometry,<sup>13–15</sup> as the most information-rich methods and amenable to clinical studies. Our research has shown that DGU has the potential for providing high precision lipoprotein density profiles by reducing error in the measurements through an understanding of how DGU works systematically and in theory and identifying the areas for which improvements are necessary. This method will be applied to clinical studies in the area of risk assessment for CVD using linear discrimination analysis (LDA).<sup>16</sup>

Density gradient ultracentrifugation has long been the gold standard for separation, identification, and quantification of lipoproteins.<sup>17–19</sup> Ultracentrifugal methods separate lipoproteins based on their hydrated densities. The different forms of this technique include rate zonal ultracentrifugation and isopycnic separations.<sup>20,21</sup> Each of these techniques has specific advantages and disadvantages including the accuracy of the separation, use in fraction preparation, and the extent of skill needed to perform these techniques. The need for a rapid and straightforward method of lipoprotein density profiling that provides the most precise information possible is therefore necessary if lipoprotein density profiles are to be used in clinical

studies. Currently, the commercialized method of lipoprotein separation through density gradient ultracentrifugation is vertical auto profiling (VAP) run by Atherotech. This method involves the use of potassium bromide (KBr) as the salt present in the aqueous gradient.<sup>22,23</sup> Use of this high ionic strength solution is problematic as it has been shown to create multicomponent aggregates of the low-density lipoproteins.<sup>24</sup> VAP results have been applied to CVD risk assessment; however, the results can vary, and the precision for an individual patient is questionable.<sup>25</sup>

Because of the inherent labor-intensive features in density-based lipoprotein separations methods, alternate methods for lipoprotein characterization have been developed. Nuclear magnetic resonance (NMR),<sup>26–28</sup> chromatographic,<sup>29,30</sup> and electrophoresis-based methods<sup>7,31,32</sup> have been explored in order to characterize lipoprotein subclasses. In these methods, it is not the hydrated density that is the defining parameter but rather the size of the lipoprotein particle or mobility inside the medium. The NMR lipoprotein profiling method is currently the most widely used in clinical applications and is able to deconvolute the lipoprotein distribution into 11 subclasses.<sup>26</sup> Risk assessment analysis using NMR has shown potential for the application of particle number instead of a cholesterol measurement for CVD prediction. This application has not shown any marked improvement over the standard methods currently in use.<sup>33,34</sup> Electrophoretic methods of lipoprotein separation include gel electrophoresis using agarose and analytical capillary isotachopheresis (ITP),<sup>31</sup> yet despite the continuing development and refinement

**Received:** July 14, 2011

**Accepted:** October 4, 2011

**Published:** October 04, 2011

of these techniques, recent review articles have identified problems in inter-relating the use of these methods for identifying individuals who have treatable early stage CVD.<sup>35</sup> Recently, a nomenclature for the lipoprotein subclasses has been proposed which we have adopted for our study.<sup>36</sup> This proposal is an important step toward unifying the lipoprotein classification system for the different methods that are being used.

The introduction of these analytical chemical screening methods into the clinical arena coupled with the vigorous interest and desire of the medical community to have a reliable and accurate method for screening for CVD has given us the motivation to determine to what extent the DGU method for lipoprotein characterization can be refined to provide a protocol that meets the requirements for lipoprotein testing to be used in the risk assessment of patients (CVD/no CVD).<sup>33</sup> Current research by our group has introduced the viability of the use of EDTA salts to control the density gradient formation process under ultracentrifugation conditions.<sup>10–12</sup> In particular, use of the NaBiEDTA complex has been shown to generate a density gradient for profiling the full density distribution of lipoproteins in 6 h rather than the 48 h required for rate zonal ultracentrifugation.<sup>11</sup> Coupling the lipoprotein density distribution separation with use of NBD C<sub>6</sub>-ceramide in order to image the intensity of the subclasses can give in principle a precise measurement of a subject's lipoprotein density profile if the precision of the measurement can be improved.<sup>12</sup> These EDTA salt solutions have a low ionic strength. This reduces the risk of aggregation in the low density lipoproteins mentioned previously. However, there is some evidence that apolipoprotein A-1 (apo A-1) loss in the high density lipoproteins could be affected by the low ionic strength.<sup>37</sup>

The objective of the study described here was to optimize the resolution and precision of the measurement of the lipoprotein density profile using the aqueous EDTA salt solution NaBiEDTA. Factors were divided into two stages. The first stage addresses those factors associated with the ultracentrifugation phase including spatial distribution of the density profile, a precise measurement of the density profile, the inherent density resolution, spin time, and temperature effects. The second stage is the imaging protocol where the fluorescently labeled density profile is converted into a digital format. Factors that were studied included the influence of the meniscus on the density profile, the stability of the density profile in the postspin time domain, contribution from light source stability, and influence of tube orientation in the imaging measurement relative to spin orientation. Through these enhancements, the goal was to develop a high precision method for lipoprotein density profiling that will determine whether the density distribution of a lipoprotein particle is a viable signature for the development of cardiovascular disease. The results obtained for the optimization studies and the final optimized method are reported here.

## EXPERIMENTAL SECTION

**Materials.** NBD C<sub>6</sub>-ceramide (6-((N-(7-nitrobenz-2-oxa-1,3-diazol-4-yl)amino)hexanoyl) sphingosine, catalog # N1154) and fluorospheres (0.1  $\mu$ m carboxylate modified red fluorescent microspheres, catalog # F-8801) were purchased from Invitrogen, Carlsbad, CA. Sodium bismuth EDTA (C<sub>10</sub>H<sub>12</sub>N<sub>2</sub>O<sub>8</sub>NaBi · 4H<sub>2</sub>O) was purchased from TCI America (Portland, Oregon). Dimethyl sulfoxide (DMSO) and hexane (>95%) were purchased from EM Science (Darmstadt, Germany). Deionized water used in all experiments was from a Milli-Q water purification system

(Millipore, Bedford, MA). Polycarbonate thick wall ultracentrifugation tubes (1.5 mL, 34 mm length, catalog # 343778) were purchased from Beckman-Coulter (Palo Alto, CA).

**Serum Collection.** The serum used for these studies was acquired from a multiple donors with informed consent. The serum was collected in a 9.5 mL Vacutainer treated with polymer gel and silica activator (366510, Beckton Dickinson Systems, Franklin Lakes, NJ). The serum was separated from the red blood cells by centrifugation at 3200 rpm for 30 min at 5 °C and then stored at –86 °C prior to use.

**Ultracentrifugation.** Ultracentrifugation was carried out using an Optima TLX ultracentrifuge and a TLA 120.2 fixed-angle rotor (Beckman-Coulter, Palo Alto, CA). Samples were spun using a rotor speed of 120 000 rpm. For the TLA120.2 rotor, these speeds correspond to average relative centrifugal force of 511 000g. A 0.1800 M solution of NaBiEDTA was selected as the initial concentration to achieve the desired density gradient profile.

**Density Gradient Measurement.** The density gradient distribution for the 0.1800 M NaBiEDTA was measured for several different spin times ranging from 2 to 8 h. The method used follows a procedure and calibration method developed by Johnson et al. where 10 aliquots (20  $\mu$ L volumes) are withdrawn from well-defined positions within the gradient and their densities are measured by refractive index.<sup>11</sup> Gradient curves were then calculated by mapping the tube coordinate versus density using Origin 7.0.

**Fluorescent Labeling of Serum Samples.** Serum samples were stained for imaging as follows: 6  $\mu$ L of serum was mixed with 10  $\mu$ L of NBD C<sub>6</sub>-ceramide (1 mg/mL in DMSO) and diluted to 1300  $\mu$ L using an aqueous solution of the density-forming solute (NaBiEDTA) followed by incubation for 30 min to achieve saturation.<sup>11,12</sup>

**Fluorescence Imaging.** Fluorescence imaging was used in monitoring the dynamics of the density gradient formation as well as the measurement of the sedimentation equilibrium density profile. An image of the tube containing the fluorophore was obtained and analyzed using a digital Optronics Microfire Camera (S99808, Goleta, CA) with a Fiber-Lite MH-100 Illuminator, a metal halide lamp, as a light source (MH100A, Edmund Industrial Optics, Barrington, NJ). A digital color microscope camera (S99808, Optronics, Goleta, CA) was used to record the image. The camera and light source were placed orthogonally to each other on an optical bench to illuminate the ultracentrifuge tube mounted in a custom-designed holder. Two filters matching the excitation and emission characteristics of the fluorophore were chosen. Specific settings for the Microfire camera software were a gain of 1.000 and a target intensity of 30% to illuminate the tube. The exposure time was optimized for sensitivity and to achieve linearity.

The image of the polycarbonate ultracentrifuge tube was then converted to a density profile following the method described by Johnson et al.<sup>11</sup> Briefly, the two-dimensional pixel field generated by the camera software was converted to a digital matrix of intensity versus tube coordinate (6–33 mm length) using Origin 7.0 software to generate a graphical representation of the density profile.

**Polar vs Nonpolar Layering.** In preliminary studies, we determined that the meniscus of the solution was interfering with the imaging of the lowest density lipoproteins. Following the UC spin, samples were layered with different liquids in order to further separate lipids or remove the meniscus from the image. Initial layering of the samples was done with 150  $\mu$ L of DI H<sub>2</sub>O

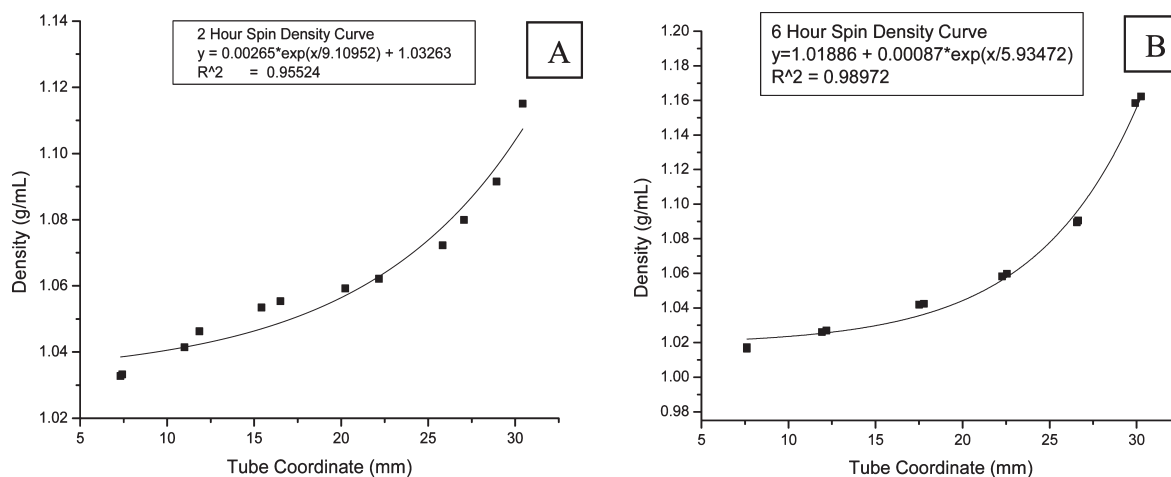


**Figure 1.** Density curve progression. (A) density curve at 2 h spin time; (B) density curve at 6 h spin time.

layered using gel loading tips (Sigma Aldrich, St. Louis, MO, catalog # CLS4853). Enhanced methods of layering use 240  $\mu\text{L}$  of hexane with gel loading tips (Sigma Aldrich, St. Louis, MO). Liquid volumes were slowly added on top of the sample without perturbing the density profile that was generated in the UC.

**Accuracy and Precision of Density Profile Measurement Using Nanospheres.** Using the fluorospheres and following the method for density gradient measurements, the accuracy and precision of the density measurement were studied. Briefly, 1  $\mu\text{L}$  of the fluorosphere solution was mixed with 1299  $\mu\text{L}$  of 0.18 M NaBiEDTA. A volume of 1150  $\mu\text{L}$  of this mixture was then spun as described above and imaged using a green excitation filter (VG-6) with a bandwidth centered at 520 nm and a red emission filter (R-60) with a low cutoff at 600 nm (Edmund Industrial Optics, Barrington, NJ).

**Lipoprotein Profiling.** Following the UC spin and layering, an image of the tube was obtained and analyzed using the method for fluorescence imaging. Two filters matching the excitation and emission characteristics of NBD C<sub>6</sub>-ceramide from Schott Glass (Elmsford, NY) were chosen. A blue-violet filter (BG-12) with a bandwidth centered at 455 nm and a yellow emission filter (OG-515) with a bandwidth centered at 570 nm were used as the excitation and emission filters, respectively. Specific settings for the Microfire camera software were an exposure of 53.3 ms with a gain of 1.000 and a target intensity of 30% to illuminate the tube prior to image capture.

**Effect of Spin Temperature on Density Profiles.** The effect of the temperature in the ultracentrifuge chamber on the lipid profiles was studied when the samples were run using the pre-described method and varying the temperature at which the samples are run. Specifically, the samples are run at 278, 288, and 298 K.

**Stability of Lipoprotein Profile after UC Spin.** Stability of the lipoprotein profile was studied by taking an initial measurement as described previously and then recording consecutive measurements every 30 min for a period of up to 90 min.

**Precision of the Lipoprotein Density Profile Measurement.** Using serum from the single donor, ten replicate measurements were made of the lipoprotein density profile. The ten profiles were overlaid to identify any systematic error in the measurement. A more quantitative and informative approach to measuring the inherent precision of the method was introduced that involves determining the integrated fluorescence intensities of the 11 subclasses based on density ranges as described in the

literature.<sup>38</sup> For each of the subclasses, the mean value and standard deviation of the intensities of each of the subclasses was evaluated. While this analysis gives an overall estimate of the precision of the measurement related to sample preparation, an additional contribution of error comes from day-to-day variability in the intensity of the light source. Consequently, we established two methods for measuring precision. The first method (referred to as Mode 1) determines the mean value and standard deviation of the absolute fluorescence intensities of each of the subclasses. The second method (Mode 2) is a normalization of data where the fluorescence intensity of each of the subclasses is given as a percent of the total integrated intensity. This approach eliminates the day-to-day variability of the light source intensity.

## RESULTS AND DISCUSSION

The long-term objective of this research is to use the EDTA gradients previously studied by our group to develop a high precision method for profiling a patient's serum using density gradient ultracentrifugation (DGU) that could be applied to clinical studies. On the basis of the previous work with EDTA gradient by Johnson et al.,<sup>11</sup> NaBiEDTA was chosen as the desired salt for manipulation of the density gradient formation because of the ability to create a gradient encompasses the density range of the lipoproteins with optimal resolution.<sup>11</sup> The developmental plan was divided into two stages. The first stage includes all factors inherent to the ultracentrifugation of the samples to separate the lipoproteins by density. The second stage focuses on factors inherent to the imaging and data analysis of the lipoprotein density profile. The overall objective of the developmental work was to convert the lipoprotein density distribution to a set of fluorescence intensities for the lipoprotein subclasses with high precision suitable for accurate classification analysis.

**Density Gradient Formation.** Understanding the formation mechanics of the density gradient allowed for the mapping of a lipoprotein profile based on density as well as a determination of the inherent resolution of the density profile. The overall precision of the density profile measurement is dependent on the precision of the density gradient that is formed. We chose to use the establishment of the sedimentation equilibrium condition as the criterion. This condition is identified by the exponential increase in solution density along the ultracentrifuge tube axis. In this study,

we determined how long it takes for the solution to achieve sedimentation equilibrium. The initial state was a homogeneous solution of 0.1800 molar NaBiEDTA. Figure 1A shows the density profile after a 2 h spin at 278 K. Superimposed on that profile is the best fit to an exponential curve showing a systematic deviation in the low density region (1.04–1.06 g/mL) and an overall data correlation  $R^2$  value of 0.955. The evolution of the profile was then extended over a period of 4–8 h spin time. At 6 h, (Figure 1B), the curve has a better fit to an exponential function with an  $R^2$  value of 0.9897. There is little change in the gradient and  $R^2$  if the spin time is extended past 6 h. From this study, we established 6 h as the standard spin time for our studies and used the equation derived from this profile to convert tube coordinate to a density coordinate. This is an important finding because it means that the attainment of sedimentation equilibrium is much faster than previously used density-forming solutes. We attribute this improvement to the properties of NaBiEDTA, a compact high molecular weight structure with low viscosity which translates to more rapid sedimentation and diffusion kinetics.

**Optimization of the Spatial Separation and Precision of the Lipoprotein Density Profile.** The initial method described previously by Johnson et al. used a 1000  $\mu\text{L}$ , 0.2000 M NaBiEDTA aqueous solution to form the gradient and deionized water ( $\text{DI H}_2\text{O}$ ) as a layering medium for separation of the chylomicrometers and TRLs that are less dense than 1.00 g/mL from the denser VLDL and TRLs.<sup>11</sup> Three factors were studied to improve the overall spatial separation and improvement of precision. The spatial separation was first expanded by increasing the volume of the solution in the ultracentrifuge tube from 1000 to 1150  $\mu\text{L}$ . In addition, the concentration of the NaBiEDTA was decreased from 0.2000 to 0.1800 M. An analysis of the precision of the fluorescence intensities of the lipoprotein subclasses showed that the precision of the low density subclasses was considerably lower. We postulated that the use of water layering to separate the meniscus from the low density fractions was the source of the problem. In the layering step, the water can mix with the aqueous gradient by convection depending upon the speed of layering which then perturbs the position of the low density subclasses in the ultracentrifuge tube. There is also an added factor due to light scattering from the meniscus at the wavelength for NBD emission from the LDL and HDL subclasses. To resolve these problems, we incorporated a nonpolar layering medium that is less dense than the lipoproteins. For this purpose, hexane was chosen as a layering medium. The volume of hexane was chosen in order to shift the meniscus away from the imaging region.

Previous literature has documented the delipidating effect that hexane can have on lipoproteins. These methods include long incubation times of 30 min at high temperatures of 60  $^\circ\text{C}$ .<sup>39</sup> The layering method applied here limits the interaction of the hexane and lipoproteins in that the hexane only interacts with the TRL portion of the lipoprotein profile due to the density separation and the time of interaction is minimal. Once a sample has been layered, it is immediately imaged. The polar nature of the aqueous gradient versus the nonpolar nature of the hexane will also limit the hexane's interaction with the lipoproteins. This limited interaction means that there will be little to no effect on the lipoprotein profile in the time needed to image.

Figure 2 shows the overlaid lipoprotein profiles for comparison of the influence of changes in the solution volume and NaBiEDTA concentration as well as the two layering methods. The peak at 6 mm for the water-layered profile is mainly the scattered light from the meniscus. For the hexane-layered profile, the meniscus is

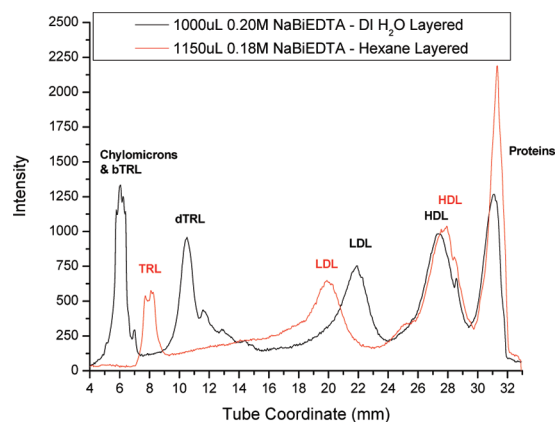


**Figure 2.** Comparison of layering methods in lipoprotein density profiles.

shifted outside of the imaging field. In addition, the convection problem associated with water layering is eliminated by hexane layering which does not penetrate into the aqueous phase. The most significant improvement in the shape of the density profile is in the TRL/LDL region where the TRL forms a sharp peak at the hexane/aqueous solution interface (8 mm tube coordinate) and the LDL region between 9 and 18 mm where the precision of the fluorescence intensities is markedly improved. The shift in tube coordinate for the LDL to a lower value is due to a change in the density profile as a result of increasing the volume of solution and decreasing the initial concentration of NaBiEDTA. The HDL and protein distributions have not been affected by these changes because they are far removed from the meniscus region.

The change seen in the protein peak of the lipoprotein profile is of no consequence to this study due to the nature of the imaging method and the shape of the UC tube. Since the UC tube is curved at the bottom, the excitation over the area is not equal, and therefore, the imaging and quantification of this area is not precise. It is also important to note that the NBD fluorophore only fluoresces in a nonpolar environment. Any free proteins in this area would not cause for fluorescence. The fluorescence in this area can be attributed to the high concentration of human serum albumin (HSA)/lipid aggregates present.

**Spin Temperature Effect on Density Profiles.** Two temperature-dependent factors are relevant to this study. The most significant relates to the structural stability of the lipoprotein particles in the sedimentation equilibrium process. A lower spin temperature promotes thermal stability. Lipoprotein density profiles were recorded at 278, 288, and 298 K using serum from the single donor. (Hexane layering was employed for imaging.) While the general forms of the density profiles were essentially the same, there was a clearly detectable shift in the density profiles toward the higher density region. We attribute this shift to the temperature dependence of the sedimentation equilibrium constant. In the sedimentation equilibrium equation, temperature is inversely proportional to the slope of the density gradient.<sup>40,41</sup> Conceptually, at the lower temperature, the diffusion rate is reduced while the sedimentation rate is not influenced by the lower temperature. The influence of temperature on the overall precision of the fluorescence intensity was significant, a factor of 2 higher at 278 K than at 298 K. On the basis of these findings, we established 278 K as the standard spin temperature for the high performance lipoprotein density measurement.

**Stability of the Lipoprotein Profile after UC Spin.** The stability of the lipoprotein density profile after the spin is completed

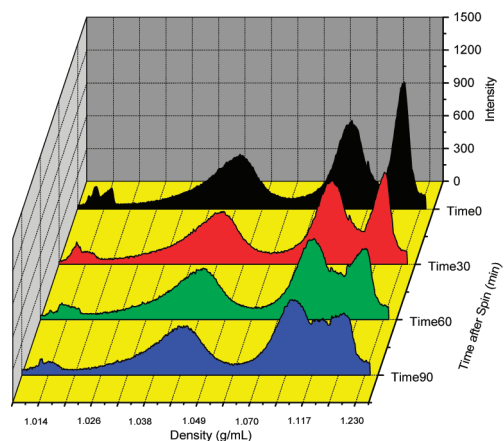


**Figure 3.** Stability of the lipoprotein density profile over time. Lipoprotein density profiles are staggered based on the amount of time after the UC spin that the image was taken.

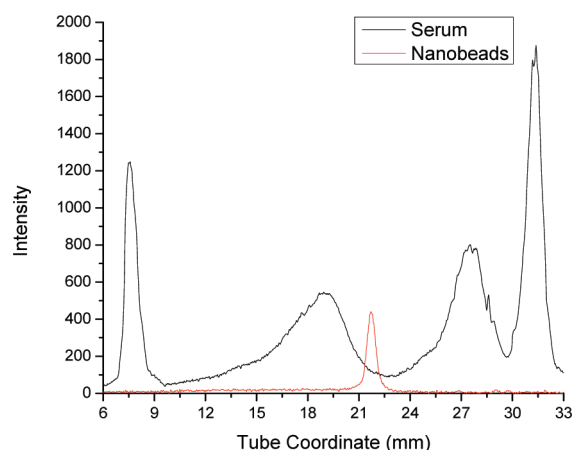


**Figure 4.** Six hour spin profiles for serum and fluorescent nanoparticles.

is an issue that has an influence on the precision of the measurement. A study was carried out where the time lapse between the end of the spin and imaging varied from 1 to 90 min. Figure 3 shows how the profile changes over time after a sample is spun, layered, and imaged. The profiles in Figure 3 have used the density curve mapped in Figure 1 to extrapolate the density relative to tube coordinate on the  $x$ -axis instead of the use of the tube coordinate scale. The figure shows that it is the high density range of the profile that is most affected by the time after spin. The protein peak separated at the high density section of the lipoprotein profile begins to merge with the HDL3 region after 30 min. The remainder of the lipoprotein profile is remarkably stable, even after 90 min. The high density component of the profile is most likely due to the density gradient starting to diffuse back to the original concentration of the aqueous solution before the UC spin. Thus, the merging peaks seen in the HDL and protein region are due to the remixing of the HDL and HSA into a heterogeneous solution. For repeatability and quality of the lipoprotein profile, the images are recorded within a few minutes after the UC spin is completed.

**Study of the Density Resolution in DGU Using a Nanoparticle Surrogate.** The class of lipoproteins covers a range of particle sizes as well as density. We selected a commercially available fluorescent nanoparticle (FluoSphere) as a model for a

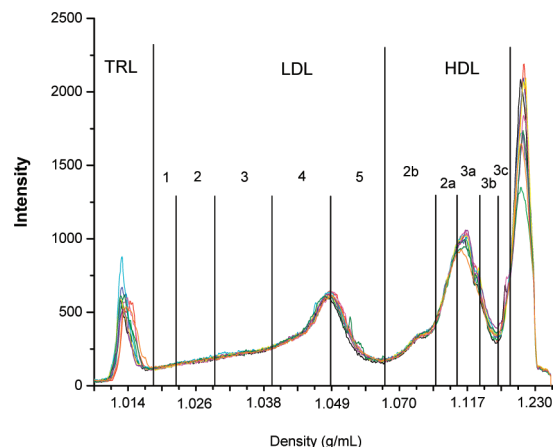


**Figure 5.** Repeatability of lipoprotein density profile.

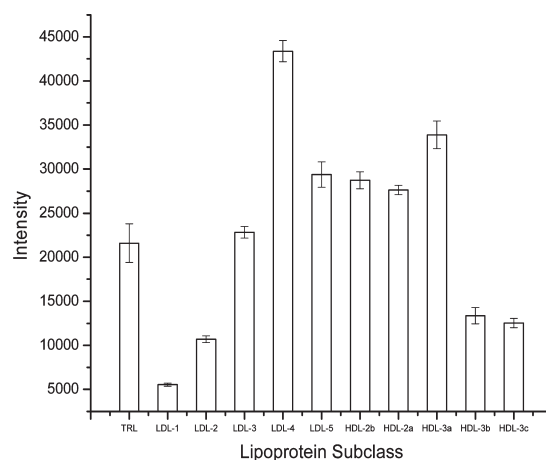


**Figure 6.** HPLDP lipoprotein subclass error for total intensity (Mode 1).

lipoprotein particle and to study the accuracy of the density measurement. It has a diameter of 100 nm and a density of 1.05 g/mL, close to the average properties of an LDL particle. Figure 4 shows the density distributions of this particle after a 6 h spin in comparison to a standard lipoprotein density profile. Using the density calibration equation for the 6 h spin, we determined that the lower limit of the density resolution ( $\Delta\rho/\rho \times 100$ ) was 0.13% at 6 h. The reported density of the FluoSpheres is 1.05 g/mL. The density of the FluoSpheres was calculated to be 1.052 g/mL. The error of the density measurement was calculated at 0.19%. The percent relative standard deviations (%RSD) of the density measurement ranged from 0.01 to 0.04% with an average of 0.027%. This accuracy and resolution shown in measuring the nanoparticle standard is also a measure of the inherent accuracy and resolution of the lipoprotein density profile.

**Precision of the Lipoprotein Density Profile Measurement.** The rationale for optimizing the precision of the lipoprotein density profile is based on the premise that a more accurate classification of individuals with and without coronary artery disease could be achieved. The platform for our developmental work was the initial method pioneered by Johnson et al., where the average %RSD was found to be 23.39%. Applying the enhancements described in this study to create the high performance lipoprotein density profiling method (HPLDP), the average %

RSD was reduced to 4.42%. The method used to determine the precision of the subclass measurements is summarized in the Experimental Section. The strategy was to obtain 10 replicate measurements of the density profile. Figure 5 shows all 10 lipoprotein density profiles overlaid from one of the volunteer's serum samples. Again, the  $x$ -axis density scale was extrapolated from the equation found in Figure 1. There are very few differences that can be distinguished between profiles. The next step was to extract from the profiles the fluorescence intensities of each of the subclasses. From this data, the mean value and %RSD for each subclass was calculated. The results are presented in histogram form shown in Figure 6 along with error bars for each subclass. The errors of the TRL and low density LDL regions of the profile are the most significantly reduced. This effect can be related to the change in layering methods. The polar–nonpolar relationship of the aqueous gradient to the hexane prevents diffusion of the layering medium and therefore reduces the error of the profile. The reduction of error in this method fits the guidelines established by the National Cholesterol Education Program that measurement of lipoproteins must meet a total error of less than 12%.<sup>42</sup> The error of the system was tested for multiple serum samples. The relative error for the different profiles was similar to the sample presented here with an average %RSD between samples of  $5.28\% \pm 0.88$ . This shows that the error between lipoprotein profiles is due to the method and not sample bias.

**Normalization of the Lipoprotein Density Profile.** An additional class of factors influencing precision is linked to the clinical study involving factors inherent in the processes of sample preparation and imaging. Examples include variability in volume of serum used, amount of fluorophore added, intensity of the light source, and factors influencing the fluorescence intensity of the subclasses. How much of the 5% overall error is due to these factors? To estimate this effect, we normalized the fluorescence intensities of each of the subclasses to the sum of the intensities of each of the subclasses. For example, the integrated intensity of the LDL-4 subclass is 42 500 (Figure 6). This intensity represents 17.4% of the total intensity of the profile. The distribution is identical in form, as expected, but the overall precision as been improved from 4.42% to 3.69%, a small, but significant improvement. Whether classification is influenced using the original data (Mode 1) or the normalized data (Mode 2) is a question that will be addressed in the application to clinical studies.

## CONCLUSIONS

We have shown here methods to reduce the error in lipoprotein profiling through understanding the mechanics of the density gradient and fluorescent imaging in order to use this technique as a tool for clinical studies in medical research. Enhanced spin volume allows for better separation of the lipoprotein profiles. Changing the layering medium reduces inherent errors present in the lipoprotein density profile. Furthermore, a proposed new systematic form of data analysis, Mode 2, shows potential for application to clinical studies. As a result of these and other techniques described in this study, a high precision method for the measurement of lipoprotein profiles (HPLDP) has been produced for application to clinical studies. This method is currently being used in ongoing clinical studies in our laboratory. Consequently, this report also serves as a detailed reference for how the lipoprotein density profile is measured for these clinical studies.

Finally, we have made a concerted effort to address the long-standing general belief that lipoproteins are unstable when

exposed to the forces of ultracentrifugation. If sedimentation were the only force, that would be the case, but sedimentation equilibrium provides a balance of sedimentation and diffusion that is so gentle that it takes 6 h for the lipoprotein particle to move a few millimeters. Further, the ionic strength of the NaBiEDTA is close to physiological levels which will allow for the measurement of lipoproteins as close to their natural state as possible. Coupled with the shorter spin time compared to the gold standard (6 h vs 48 h) and reduced temperature (278 K vs room temperature), we are confident that lipoprotein density profile measured by this method has the precision to determine whether it can be used to obtain a more accurate classification of subjects at risk for CVD. This feature is the overall objective for the development of this method. Other factors besides density could be contributing to the classification. Subject variability in the uptake and fluorescence of the NBD ceramide as well as the stability of the lipoproteins under DGU conditions may actually contribute to the distinction between subjects and will therefore aid in the classification of risk.

## AUTHOR INFORMATION

### Corresponding Author

\*E-mail: macfarlane@mail.chem.tamu.edu. Phone: (979) 845-2021. Fax: (979) 845-8987.

## ACKNOWLEDGMENT

This work was supported by the NIH Heart, Lung and Blood Institute RO1HL068794.

## REFERENCES

- (1) Enriquez, J. R.; De Lemos, J. A. *Prev. Cardiol.* **2010**, *13*, 152.
- (2) Ikonomidis, I.; Michalakeas, C. A.; Lekakis, J.; Paraskevaidis, I.; Kremastinos, D. T. *Dis. Markers* **2009**, *26*, 273.
- (3) Kim, H. C.; Greenland, P.; Rossouw, J. E.; Manson, J. E.; Cochrane, B. B.; Lasser, N. L.; Limacher, M. C.; Lloyd-Jones, D. M.; Margolis, K. L.; Robinson, J. G. *J. Am. Coll. Cardiol.* **2010**, *55*, 2080.
- (4) Lakić, D.; Bogavac-Stanojević, N.; Jelić-Ivanović, Z.; Kotur-Stevuljević, J.; Spasić, S.; Kos, M. *Value Health* **2010**, *13*, 770.
- (5) Schnabel, R. B.; Schulz, A.; Messow, C. M.; Lubos, E.; Wild, P. S.; Zeller, T.; Sinning, C. R.; Rupprecht, H. J.; Bickel, C.; Peetz, D.; Cambien, F.; Kempf, T.; Wollert, K. C.; Benjamin, E. J.; Lackner, K. J.; Munzel, T. F.; Tiret, L.; Vasan, R. S.; Blankenberg, S. *Eur. Heart J.* **2010**, *31*, 3024.
- (6) Cruzado, I. D.; Song, S. Q.; Crouse, S. F.; O'Brien, B. C.; Macfarlane, R. D. *Anal. Biochem.* **1996**, *243*, 100.
- (7) Hu, A. Z.; Cruzado, I. D.; Hill, J. W.; McNeal, C. J.; Macfarlane, R. D. *J. Chromatogr., A* **1995**, *717*, 33.
- (8) Macfarlane, R. D.; Bondarenko, P. V.; Cockrill, S. L.; Cruzado, I. D.; Koss, W.; McNeal, C. J.; Spiekerman, A. M.; Watkins, L. K. *Electrophoresis* **1997**, *18*, 1796.
- (9) Chandra, R.; Macfarlane, R. D. *Anal. Chem.* **2006**, *78*, 680.
- (10) Hosken, B. D.; Cockrill, S. L.; Macfarlane, R. D. *Anal. Chem.* **2005**, *77*, 200.
- (11) Johnson, J. D.; Bell, N. J.; Donahoe, E. L.; Macfarlane, R. D. *Anal. Chem.* **2005**, *77*, 7054.
- (12) Henriquez, R. R.; Chandra, R.; Hosken, B.; Macfarlane, R. D. *Atheroscler. Suppl.* **2006**, *7*, ThP17428.
- (13) Bondarenko, R.; Farwig, Z. N.; McNeal, C. J.; Macfarlane, R. D. *Int. J. Mass Spectrom.* **2002**, *219*, 671.
- (14) Moore, D.; McNeal, C.; Macfarlane, R. *Biochem. Biophys. Res. Commun.* **2011**, *404*, 1034.
- (15) Johnson, J. D.; Henriquez, R. R.; Tichy, S. E.; Russell, D. H.; McNeal, C. J.; Macfarlane, R. D. *Int. J. Mass Spectrom.* **2007**, *268*, 227.

- (16) Lavie, C. J.; Milani, R. V. *Prog. Cardiovasc. Dis.*, **53**, 397.
- (17) Work, T. S., Work, E., Eds. *Laboratory Techniques in Biochemistry and Molecular Biology*; Elsevier: Amsterdam, 1978; Vol. 6, p 97.
- (18) Hoinacki, J. L.; Nicolosi, R. J.; Hoover, G.; Llansa, N.; Ershow, A. G.; Lozy, M. e.; Hayes, K. C. *Anal. Biochem.* **1978**, *88*, 485.
- (19) Laker, M. F.; Game, F. L. *Baillieres Clin. Endocrinol. Metab.* **1990**, *4*, 693.
- (20) Johnson, C.; Attridge, T.; Smith, H. *Biochim. Biophys. Acta (BBA)-Protein Struct.* **1973**, *317*, 219.
- (21) Fourcroy, P. *Biochem. Biophys. Res. Commun.* **1978**, *84*, 713.
- (22) Archer, E.; Blair, S. N. *Prog. Cardiovasc. Dis.*, **53**, 387.
- (23) Vancraeynest, D.; Pasquet, A.; Roelants, V.; Gerber, B. L.; Vanoverschelde, J.-L. J. *J. Am. Coll. Cardiol.* **2011**, *57*, 1961.
- (24) Biondi-Zoccai, G.; Romagnoli, E.; Agostoni, P.; Capodanno, D.; Castagno, D.; D'Ascenzo, F.; Sangiorgi, G.; Modena, M. G. *Contemp. Clin. Trials* **2011**, *32*, 731.
- (25) Lavie, C. J.; Milani, R. V.; O'Keefe, J. H.; Lavie, T. J. *Prog. Cardiovasc. Dis.*, **53**, 464.
- (26) Ala-Korpela, M.; Lankinen, N.; Salminen, A.; Suna, T.; Soininen, P.; Laatikainen, R.; Ingman, P.; Jauhiainen, M.; Taskinen, M.-R.; Héberger, K.; Kaski, K. *Atherosclerosis* **2007**, *190*, 352.
- (27) Dyrby, M.; Petersen, M.; Whittaker, A. K.; Lambert, L.; Nørgaard, L.; Bro, R.; Engelsen, S. B. *Anal. Chim. Acta* **2005**, *531*, 209.
- (28) Hodge, A. M.; Jenkins, A. J.; English, D. R.; O'Dea, K.; Giles, G. G. *Diabetes Res. Clin. Pract.* **2009**, *83*, 132.
- (29) Legget, M. E.; Ellis, C. J.; Edwards, C.; Van Pelt, N.; Ormiston, J. A.; Christiansen, J.; Winch, H.; Young, R.; Gamble, G. *Heart, Lung Circ.* **2011**, *20*, 391.
- (30) Ellis, C. J.; Legget, M. E.; Edwards, C.; Van Pelt, N.; Gabriel, R.; Ormiston, J. A.; Christiansen, J.; Winch, H.; Osborne, M.; Gamble, G. *Heart, Lung Circ.* **2011**, *20*, 383.
- (31) Schmitz, G.; Möllers, C.; Richter, V. *Electrophoresis* **1997**, *18*, 1807.
- (32) Stocks, J.; Miller, N. E. *Electrophoresis* **1999**, *20*, 2118.
- (33) Bhupathiraju, S. N.; Tucker, K. L. *Clin. Chim. Acta* **2011**, *412*, 1493.
- (34) Moran, A.; DeGennaro, V.; Ferrante, D.; Coxson, P. G.; Palmas, W.; Mejia, R.; Perez-Stable, E. J.; Goldman, L. *Int. J. Cardiol.* **2011**, *150*, 332.
- (35) Ensign, W.; Hill, N.; Heward, C. B. *Clin. Chem.* **2006**, *52*, 1722.
- (36) Rosenson, R. S.; Brewer, H. B., Jr.; Chapman, M. J.; Fazio, S.; Hussain, M. M.; Kontush, A.; Krauss, R. M.; Otvos, J. D.; Remaley, A. T.; Schaefer, E. J. *Clin. Chem.* **2011**, *57*, 392.
- (37) Kulkarni, K. R. *Clinics Lab. Med.* **2006**, *26*, 787.
- (38) Ikeda, T.; Seo, M.; Inoue, I.; Katayama, S.; Matsunaga, T.; Hara, A.; Komoda, T.; Tabuchi, M. *Anal. Chem.* **2009**, *82*, 1128.
- (39) Okwuosa, T. M.; Greenland, P.; Ning, H.; Liu, K.; Bild, D. E.; Burke, G. L.; Eng, J.; Lloyd-Jones, D. M. *J. Am. Coll. Cardiol.* **2011**, *57*, 1838.
- (40) Cole, J. L.; Lary, J. W.; Moody, P. T.; Laue, T. M. In *Methods in Cell Biology*; Correia, J. J., Detrich, H. W., III, Eds.; Academic Press: London, 2008; Vol. 84, p 143.
- (41) Milthorpe, B. K.; Jeffrey, P. D.; Nichol, L. W. *Biophys. Chem.* **1975**, *3*, 169.
- (42) *Recommendations on lipoprotein measurement from the Working Group on Lipoprotein Measurement*; National Institutes of Health, National Heart, Lung and Blood Institute: Bethesda, MD, 1995.